

# Covalent Conjugate of Ser-Pro-Cys Tripeptide with PEGylated Comb-Like Polymer as Novel Killer of Human Tumor Cells

Nazar Manko, Marina Starykovich, Nataliya Mitina, Kateryna Volianiuk, Lizhen Wang, Meng Jin, Kechun Liu, Rostyslav Panchuk, Olga Klyuchivska, Alexander Zaichenko, Yuriy Kit, and Rostyslav Stoika\*



Cite This: *ACS Omega* 2022, 7, 41956–41967



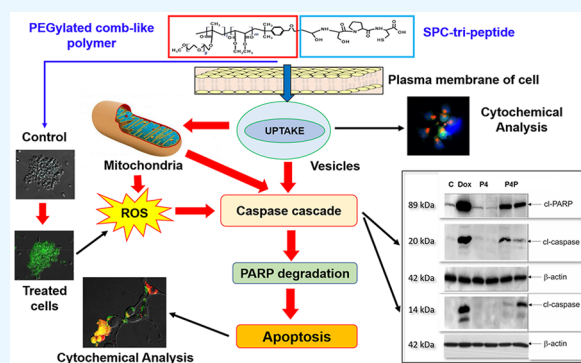
Read Online

ACCESS |

Metrics & More

Article Recommendations

**ABSTRACT:** Recently, we detected a previously unknown Ser-Pro-Cys (SPC) tripeptide in the blood serum of multiple sclerosis patients. Its role as a biomarker of the autoimmune disease was suggested, although its origin and real biological activity remained unclear. Here, we created a biocompatible PEGylated comb-like polymer that was used as a platform for covalent immobilization of the SPC, which provided a possibility to explore the biological activity of this tripeptide. This macromolecular conjugate was synthesized via a reaction of the terminal epoxide group of the biocompatible copolymer of dimethyl maleate (DMM) and polyethylene glycol methyl ether methacrylate (PEGMA) with the amino group of the SPC tripeptide. Unexpectedly, the resulting conjugate containing SPC demonstrated anticancer activity *in vitro*. It possessed pro-apoptotic action toward human tumor cells, while there was no cytotoxic effect of that conjugate toward normal lymphocytes of human peripheral blood. The detected biological effects of the created conjugate inspired us to carry out a thorough study of structural and colloidal-chemical characteristics of this surface-active copolymer containing side PEG chains and a terminal nontoxic synthetic fragment. The copolymer composition, in particular, the content of the peptide fragment, was determined via elemental analysis and NMR spectroscopy. At CMC, it formed polymeric micelle-like structures with a hydrodynamic diameter of  $180 \pm 60$  nm. The conjugation of the peptide fragment to the initial comb-like copolymer caused a change of zeta-potential of the formed micelle-like structures from  $-0.15$  to  $0.32$  mV. Additional structural modification of the created polymeric nanoplatform was performed via attachment of fluorescein isothiocyanate (FITC) dye that permitted monitoring of the behavior of the bioactive SPC-functionalized conjugate in the treated tumor cells. Its penetration into those cells and localization in their cytoplasm were revealed. The principal novelty of this study consists in finding that covalent conjugation of two nontoxic compounds—SPC tripeptide and comb-like PEGylated polymer—led to an unexpected synergy which appeared in the distinct cytotoxic action of the macromolecular complex toward human tumor cells. A potential role of peculiarities of the colloidal-chemical properties of the novel conjugate in its cytotoxic effect are discussed. Thus, synthesized comb-like PEGylated polymers can provide a prospective nanoplatform for drug delivery in anticancer chemotherapy.



## INTRODUCTION

The development of novel multifunctional nanomedicines with enhanced anticancer action, reduced negative side effects, and improved physical-chemical characteristics providing water solubility to poorly soluble anticancer drugs is an important trend in the modern pharmaceutical industry.<sup>1,2,6–8</sup> Natural and synthetic polymers are the most popular nanocarriers applied for delivery of the anticancer drugs, including water insoluble ones. Such nanocarriers can also secure targeted delivery and stimuli-responsive action of anticancer drugs,<sup>3</sup> as well as a possibility for circumventing an acquired drug resistance.<sup>4</sup> PEGylated and polyoxazoline-containing polymeric carriers with low general toxicity *in vivo* are of specific interest,<sup>2,3,4</sup> and

many of them reached different stages of the preclinical and clinical trials.<sup>2</sup>

The availability of terminal or side reactive fragments in the structure of such polymeric carriers opens a possibility for covalent and noncovalent binding of various molecules of natural origin—saccharides, proteins, enzymes, oligopeptides, and oligonucleotides—and for the development of novel

Received: June 9, 2022

Accepted: October 28, 2022

Published: November 11, 2022



hybrid polymeric carriers of a desired architecture and controlled bioactivity.<sup>4</sup>

Among hybrid polymeric carriers, the peptide–polymer conjugates represent a new class of soft materials composed of covalently linked blocks of protein/polypeptides and synthetic/natural polymers.<sup>3–5</sup> Bradykinin, a natural biologically active peptide consisting of 9 amino acids, was conjugated via a hydrazone bond cleavable in acid microenvironment, with a novel N-(2-hydroxypropyl) methacrylamide (HPMA)-based copolymer.<sup>5</sup> In a conjugate with this polymer, bradykinin improved the tumor-selective action of the nanomedicine containing doxorubicin and its accumulation in tumors. Pretreatment with such a conjugate also improved the blood flow in tumors and increased the accumulation of nanomedicine in tumors that resulted in enhanced suppression of tumor development. Thus, bradykinin immobilized on the created polymer can serve as a concomitant drug that improves the delivery of nanomedicines in tumors.

It was shown that the efficiency of anticancer action of doxorubicin conjugates with comb-like pHPMA significantly depended upon the length of the backbone and side chains, as well as on drug location on the polymer.<sup>6</sup> These structural factors also affected the uptake of the nanomedicine by tumor cells, its circulation in blood, and accumulation in tumors.

Recently, we developed the biocompatible polymeric carriers composed of the PEGylated comb-like polymers which were used for transportation *in vitro* and *in vivo* of traditional (doxorubicine) and experimental (4-tiazolidinone derivatives) drugs. These nanocarriers possessed low toxicity *in vitro* toward human tumor cells of different lines, and they did not demonstrate significant toxicity (grade 4) in laboratory mice. The complexation of those polymers with doxorubicine or 4-tiazolidinone derivatives enhanced their cytotoxicity toward tumor cells *in vitro* and *in vivo*.<sup>7</sup>

We first detected and isolated previously unknown Ser-Pro-Cys (SPC) tripeptides in blood serum of the multiple sclerosis patients.<sup>1</sup> However, the origin and biological activity of this peptide remained unknown. Here, we covalently conjugated the SPC tripeptide with the PEGylated comb-like polymer (see [Experimental Section](#)). That resulted in the formation of a surface-active comb-like copolymer consisting of the backbone containing side PEG chains and a terminal SPC tripeptide fragment. Unexpectedly, such a nanoconjugate demonstrated cytotoxic action toward human tumor cells and induced their apoptosis. Due to fluorescent labeling with FITC of the created polymer conjugate with the SPC tripeptide, it was possible to demonstrate its penetration into human tumor cells and accumulation in the cytoplasm. In this study, the interrelations between structural and colloidal-chemical characteristics (hydrodynamic diameter, zeta-potential, and others) of the synthesized nanoconjugate were considered, and peculiarities of the biological action of this polymeric conjugate were characterized.

Altogether, the obtained results permitted us to promote the comb-like PEGylated copolymer as a prospective nanoplatform for drug delivery in anticancer chemotherapy. We also suggest that the created conjugate with the SPC tripeptide might be a new peptide-based inhibitor of growth of tumor cells.

## ■ EXPERIMENTAL SECTION

**Synthesis of SPC-Bearing PEGylated Comb-Like Polymer.** *Reagents.* Dimethyl maleate (DMM) (Acros, United States) was used after purification by distillation in

vacuum. Polyethylene glycol methyl ether methacrylate (PEGMA,  $M_n = 475$  Da) and azobis(isobutyronitrile) (AIBN) were obtained from Sigma-Aldrich Co. (USA) and used without additional purification. A derivative of isopropyl benzene: 2-[(4-isopropyl benzyl)oxi] methyl}oxirane (cumene glycidyl ether, CGE) was synthesized from isopropyl benzene and used without additional purification.

**Ser-Pro-Cys tripeptide** was obtained from Cellmano Biotech Ltd. (China). It was prepared via solid phase synthesis with 99.26% final purity (Lot No. 181102-P013842). We thank Prof. Liu Kechun for purchasing the Ser-Pro-Cys tripeptide used in this study.

**Procedures.** Procedures, described earlier,<sup>8–10</sup> were used to obtain a micelle-forming surface-active copolymer consisting of the backbone of the PEGylated comb-like polymer and the terminal fragment of the SPC tripeptide.

At the first stage, the comb-like copolymer poly(PEGMA-co-DMM)-CGE (P4) was synthesized via copolymerization of DMM with PEGMA initiated by the AIBN in the presence of CGE used as chain transfer agent in the dioxane at 60 °C until 65% conversion of the monomers.<sup>11</sup> A mixture of PEGMA (3.8 mL, 8.0 mmol) and DMM (0.13 mL, 0.9 mmol) and 10 mL of the CGE (0.03 mL, 0.3 mmol) was prepared; after that, an AIBN (0.1 g, 0.61 mmol) solution in the dioxane (Acros, USA) was added to the mixture. Monomer conversion was controlled via dilatometric study.<sup>9</sup> After polymerization was finished, the polymer was purified by precipitation and dried under vacuum until constant weight.<sup>10</sup> A residual PEGMA was removed by dialysis using dialysis bags with pore sizes MWCO 6 kDa (Sigma-Aldrich, USA).

At the second stage, the SPC-bearing copolymer was obtained via interaction of the peptide-NH<sub>2</sub> group with a terminal epoxide group of comb-like P4 copolymer (polymer:peptide ratio = 1:1.1 mol) at 25 °C in aqueous solution with stirring for 10 h. To remove water, the sample was dried under vacuum until constant weight was achieved. Then, the dried sample was dissolved in the bidistilled water to reach the final concentration of 16.5 mg/mL. The unreacted SPC-peptide was removed for 5 days using dialysis bags with pore size of molecular weight cutoff (MWCO) of 3.5 kDa (Sigma-Aldrich, USA).

The composition of the P4 polymer was calculated from the results of elemental analysis.<sup>8</sup> The content of terminal CGE fragments in the P4 was determined from results of measurement of epoxide groups via back-titration of the residual HCl with KOH.<sup>10</sup> <sup>1</sup>H NMR spectra were recorded on a Bruker Avance DPX 300 spectrometer at 300.13 MHz. NMR spectra of the boules were recorded in a Bruker Avance DPX 300 at the working frequency of 300.13 MHz from a D<sub>2</sub>O solution. Content of the peptide in copolymer molecules was determined using NMR spectroscopy ([Figure 2](#)).<sup>12</sup> The molecular weights of the initial and resulting polymers were determined using the size exclusion chromatography method on a Waters 150C chromatograph with a built-in RI detector (Waters Corporation, Milford, MA, USA) and a Shodex 602 column (Kawasaki, Japan). The formation of conjugates was confirmed using the NMR spectroscopy method.

The sizes of the micelles formed by P4 and P4P were measured using dynamic light scattering (DLS) on a DynaProNanoStar (Wyatt Technology, Santa Barbara, CA, USA) and Zetasizer Nano ZS (Malvern Instruments GmbH, Stuttgart, Germany) instruments. For measuring photon correlation spectra, the NIBS (Non-Invasive Back Scatter)

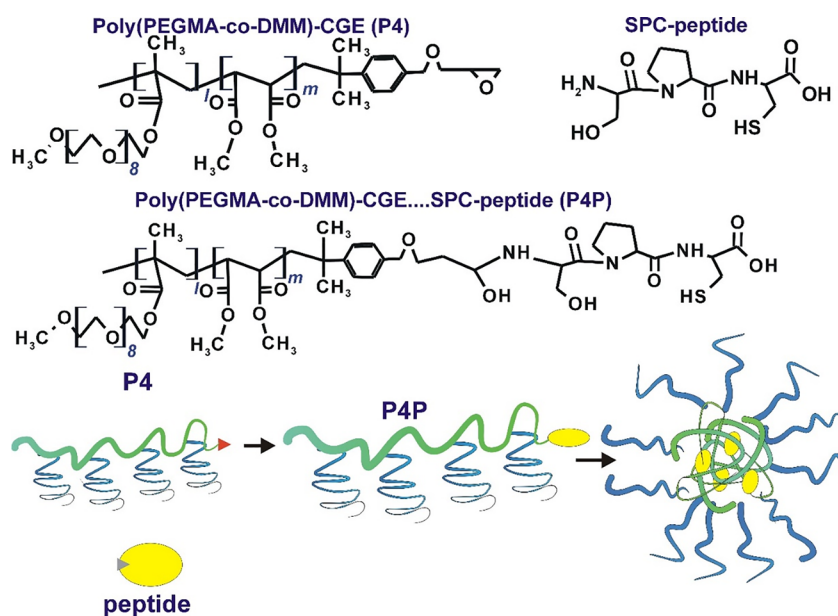


**Figure 1.** Scheme of synthesis of conjugate of the SPC tripeptide with created copolymer.

technology at 25 °C was applied. Measurements of zeta-potential were carried out with a Zetasizer Nano ZS at a fixed temperature of 25 °C.

A secondary amino group of the peptide–polymer conjugate (P4P) (Figure 1) was used to couple fluorescent dye 5(6)-isothiocyanate (FITC, Sigma-Aldrich, USA) for obtaining FITC-labeled conjugate (P4P-FITC). The synthesis was carried out in the dimethyl sulfoxide (DMSO, Merck, Germany) at 40 °C. To 1.4 mL of P4P solution (70 mg/mL) in DMSO, 2.5 mg of FITC and 8 mg of dibutyltindilaurate (DBTDL, Sigma-Aldrich, USA) were added. The mixture was stirred for 12 h; then DMSO was partially removed by distillation on a water-jet pump, and 6 mL of the bidistilled water was added. The unreacted FITC and DMSO were disposed using dialysis bags with pore size of 6–8 kDa molecular weight cutoff (MWCO). Dialysis was carried out until the disappearance of FITC luminescence was detected in dialysis water under its irradiation with a UV lamp with  $\lambda = 365$  nm (Spectroline, Spectronics Co., USA).

**Cell Culture.** Human breast carcinoma MCF-7 cells, human colon carcinoma HCT116 cells, human embryonic kidney HEK293 cells, and lymphocytes of human peripheral blood were used for cytotoxicity study. Cell lines were obtained from the Cell Culture Collection at the Institute of Molecular Biology and Genetics, National Academy of Science of Ukraine (Kyiv, Ukraine). The cells were cultured in Dulbecco's modified Eagle's medium (DMEM, Sigma, USA) supplemented with 10% fetal bovine serum (Sigma, USA). Cells were grown in a CO<sub>2</sub>-incubator at 37 °C, 5% CO<sub>2</sub>, and 95% humidity, and their reseeding was performed in 2–3 days at 1:5 ratio.

**Isolation of Normal Lymphocytes from Human Peripheral Blood and Their Activation.** Twenty milliliters of venous blood was taken from human volunteers (Bio-Ethical Protocol No 2, 27.01.2019, approved by the Bio-Ethical Commission of the Institute of Cell Biology, NAS of Ukraine) and collected in the presence of 200  $\mu$ L of undiluted fresh heparin (1/100). Fresh blood was diluted twice with 0.9% NaCl under sterile conditions. Isolation of lymphocytes (mononuclear cells) was performed in a density gradient of Ficol-Verografin, using the

manufacturer's protocol (Lymphoprep, NYCOMED PHARMA AS, Oslo Norway). The resulting lymphocytes were suspended in the RPMI-1640 medium and cultured for several days (up to 5 days). To separate the lymphocytes from the monocytes, the cell suspension was left for 24 h. After 24 h, the monocytes were attached, while the lymphocytes were transferred to a fresh Falcon tube (15 mL). Stimulation of growth and proliferation of lymphocytes were performed via their culturing on CD3 antibody-coated plastic plate in the RPMI-1640 medium supplemented with 20% fetal bovine serum (FBS).

**Evaluation of Antiproliferative Activity of Studied Substances.** *In vitro* screening of anticancer activity of compounds toward tumor and pseudonormal cell lines and human blood lymphocytes was measured by the MTT-testing with 3-(4,5-dimethylthiazol-2-yl)-2,5-diphenyltetrazolium bromide dye (Sigma-Aldrich, USA). Tumor cells were seeded for 24 h in 96-well plates in 100  $\mu$ L at a concentration of 5000 cells/well. After that, cells were incubated for the next 72 h with various additions. MTT was added to the studied cells according to the manufacturer's protocol (Sigma-Aldrich, USA). The purple product of the reaction (formazan crystals dissolved in the DMSO) was quantitatively measured at 630 nm wavelength in a multichannel Absorbance Reader BioTek ELx800 (BioTek Instruments, Inc., USA).

**Fluorescence Microscopy of MCF-7 Cells Treated with Studied Substances.** Observation of the alive and dead cells was performed under Mik-Med-12 microscope (LOMO, St. Petersburg, Russian Federation) at 400 $\times$  magnification. Hoechst 33342 fluorescent dye (final concentration of 0.5  $\mu$ g/mL) exhibits the excitation wavelength of 320–390 nm and the emission wavelength –420–480 nm, while the neutral red dye (final concentration of  $\sim$  0.1 mg/mL) possesses excitation at 550–600 nm and emission at 750 nm. The tested conjugate labeled with FITC was added to cultured wells according to the experimental schemes and incubated for 2, 4, and 6 h. Fluorochromes were added to cultured cells 20–30 min before the end of the experiment. Under these conditions, the cells differed in the contours or shape and the morphology of the nuclei. Images were obtained on a Carl Zeiss AxioImager A1 fluorescence microscope (Germany) equipped with a Carl



**Table 1. Structural and Molecular Weight Characteristics of Copolymers**

Composition, % mol				Molecular weight characteristics		Characteristics of micelle-like structures	
PEGMA	DMM	CGE-fragment	SPC-peptide-fragment	$M_n$ , kDa	Molecular weight distribution (MWD)	An average hydrodynamic diameter, nm	Zeta-potential, mV
68.5	25.3	6.2	-	8.2	2.21	150 ± 41	-0.15
68.0	25.0	-	7.0	7.9	2.05	180 ± 60	0.32

Zeiss AxioCamMRm camera (Germany) at appropriate excitation and emission wavelengths to detect fluorescence.

FITC-Annexin V fluorescent dye (final concentration of 0.5  $\mu\text{g}/\text{mL}$ ) exhibits the excitation wavelength at 450–480 nm and the emission wavelength at 510–520 nm, while the propidium iodide (final concentration of  $\sim 0.1$  mg/mL) possesses the excitation at 550–600 nm and the emission at 650–700 nm.

**Flow Cytometry.** For apoptosis study, HL60 and Jurkat T-cell lines treated with various agents were washed with phosphate buffered saline (PBS, pH 7.4), pelleted by centrifugation at 200 g for 5 min at 4 °C, and resuspended in cold PBS (2,000,000 cells per 1 mL of the PBS). Then, cells were fixed via dropwise addition of cooled ( $-20$  °C) absolute ethanol (total volume 4 mL) with gentle mixing. The obtained samples were kept at  $-20$  °C until use (no longer than 1 week). For FACS analysis, cell samples were centrifuged for 5 min at 4 °C and 200 g, the supernatant was discarded, and the cell pellet was suspended in 1 mL of the PBS. 100  $\mu\text{L}$  of DNAase free RNAase A (Sigma) was added to that suspension, and samples were incubated for 30 min at 37 °C. Then, each sample was supplemented with 100  $\mu\text{L}$  of the propidium iodide (Sigma, 1 mg/mL) and incubated for 10 min at room temperature. The samples were transferred to plastic Falcon tubes, and cell suspension was monitored on the FACS Calibur flow cytometer (BD Biosciences, Mountain View, CA, USA). Summit v 3.1 software (Cytomation, Inc., Fort Collins, CO, USA) was used for measuring apoptosis parameters.

For measurement of the Annexin V-positive (apoptotic) cells by means of FACS analysis, HL60 and Jurkat T-cells were treated, as indicated in the figure legends, washed twice with the PBS, and stained with Annexin V-FITC using Apoptosis Detection Kit (BD Pharmingen, San Diego, CA, USA) according to the manufacturer's instructions. In particular, washed cells were incubated for 15 min in the Annexin V binding buffer containing 1/50 volume of FITC-conjugated Annexin V solution. Then, the samples were diluted twice with an appropriate volume of the Annexin V binding buffer and immediately measured on FL1/FL2 (FITC-PI) channel of the flow cytometer (Becton Dickinson, Franklin Lakes, NJ, USA). Single Annexin V-positive cells were classified as apoptotic.

**Western Blot Analysis of Apoptosis-Related Proteins.** Cellular proteins were extracted with lysis buffer (20 mM Tris-HCl, pH 8.0, 1% Triton-X100, 150 mM NaCl, 50 mM NaF, 0.1% SDS) containing 1 mM phenylmethanesulfonyl fluoride (PMSF) and 10  $\mu\text{g}/\text{mL}$  of protease inhibitors cocktail "Complete" (Basel, Roche, Switzerland), subjected to SDS-electrophoresis in 12–15% PAGE, and transferred onto the nitrocellulose membrane. The membrane was blocked with 3% BSA for 1 h at 23 °C, washed with PBST buffer (PBS with Tween-20) three times for 5 min each wash, and incubated overnight with primary human antibody (Biotechne, USA, 0.1  $\mu\text{g}/\text{mL}$ ) in 5% BSA supplemented with PBST. After incubation, the blotted membrane was washed in the PBST three times for 5 min each wash and incubated for 1.5 h with HRP-conjugated anti-mouse IgG Ab (Cell Signaling Technol-

ogy Europe, The Netherlands). Proteins transferred on the blot were visualized with ECL reagent (Sigma).<sup>13</sup> If there was no possibility to make protein detection on one blot, like with cleaved caspase 6 or cleaved caspase 7, the experiment was repeated using the same biological samples.

**Localization of the Engulfed P4P Conjugate in Human Cells in Vitro.** MCF-7 cells ( $1 \times 10^5$  cells per ml) were grown for 2 h on the cover slides in a 12-well plate; after that, a polymeric preparation with a FITC-labeled peptide was added to cells and incubated for 2 h. Then, the cells were washed with the PBS to remove the culture medium and the compound. Slides with cells were removed from the wells and analyzed under a Carl Zeiss AxioImager A1 fluorescence microscope (Carl Zeiss, Germany) equipped with a Carl Zeiss AxioCamMRm camera (Carl Zeiss, Germany) at appropriate excitation and emission wavelengths used to detect fluorescence.

**Measurement of ROS in MCF-7 Cells.** For ROS measurement, 2,7-dichlorofluorescein diacetate (DCFDA, detects mainly  $\text{H}_2\text{O}_2$ ) was used as a fluorescent probe. ROS content was measured with FACS flow cytometer (BD Biosciences, Mountain View, CA, USA) in control (untreated) cells or in cells treated for 30 min at 37 °C with P4P conjugate after cell staining with fluorescent probes (10 mM). MCF-7 cells were grown on glass slides, treated with peptide or PBS (control), and then incubated with 10 mM DCFDA for 30 min at 37 °C. After incubation was finished, cells were immediately examined under the fluorescence microscope Zeiss Axio Imager A1 (Carl Zeiss, Germany) at the wavelength Ex/Em = 495 nm/529 nm. The cells examined with Zeiss AxioLamA1 (Carl Zeiss, Germany) microscope were photographed with a digital camera (see above).

**Statistical Analysis.** All experiments were conducted three times with three parallel repeats. The Analysis of Variance (ANOVA) was used as a statistical test for the comparison of the experimental groups. Two-way ANOVA with Bonferroni post-tests was applied in order to compare replicated means by rows using GraphPad Prism v 6.0 software.

## RESULTS AND DISCUSSION

**Synthesis and Characterization of Copolymer Conjugated with SPC Tripeptide.** Synthesis of the comb-like copolymer was conducted, as described earlier.<sup>8–10</sup> In Figure 1, a scheme of its conjugation with the SPC tripeptide is presented.

As one can see (Figure 1, Table 1), the resulting copolymer consists of the block of polymer containing alternated links of DMM and PEGMA with side PEG chains along the backbone and terminal covalently conjugated SPC tripeptide. The comb-like copolymer poly(PEGMA-co-DMM)-CGE (P4) was synthesized via copolymerization of DMM with PEGMA initiated by the AIBN in the presence of CGE used as chain transfer agent.<sup>12</sup> An availability of terminal epoxide group of comb-like copolymer provides a possibility for interaction with the peptide-NH<sub>2</sub> group and the formation of the SPC-bearing



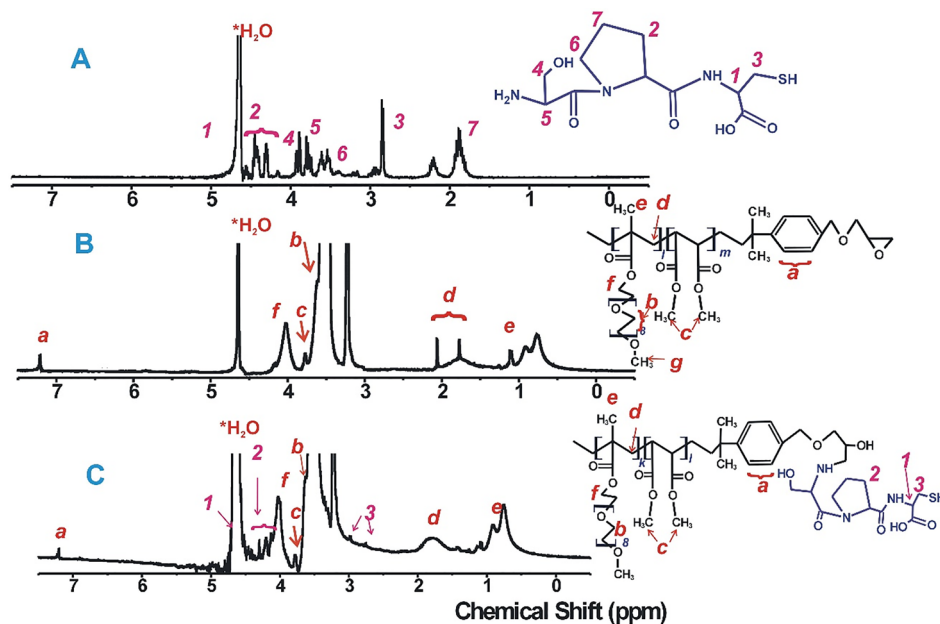


**Figure 2.** <sup>1</sup>H NMR spectra of the SPS-peptide (A), the P4 polymer (B), and P4P comb-like copolymer (C).

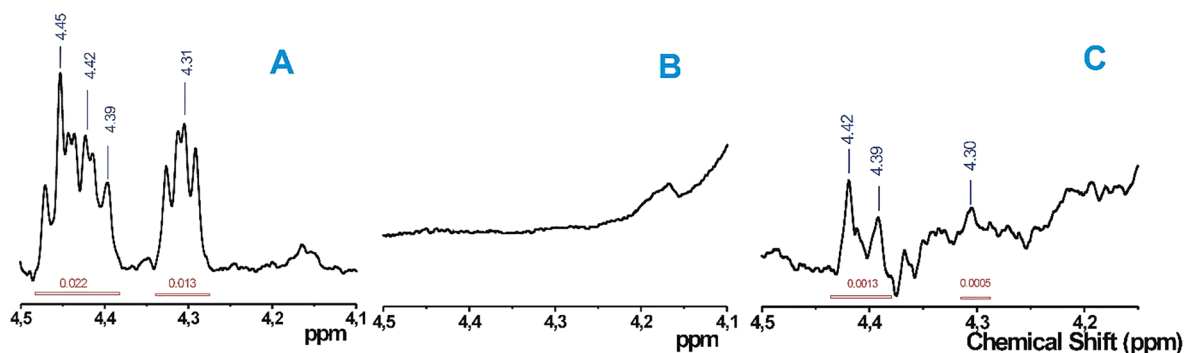


**Figure 3.** Fragment of the <sup>1</sup>H NMR spectrum of the SPS-peptide (A), P4 (B), and P4P (C) (solvent D<sub>2</sub>O).

copolymer. A secondary amino group of the peptide–polymer conjugate (P4P) was used to couple fluorescent molecule of 5(6)-isothiocyanate (FITC, Sigma-Aldrich, USA) for obtaining FITC-labeled conjugate (P4P-FITC).

In Table 1, the composition and molecular weight of the initial and resulting copolymers are presented. Data of the NMR spectra (Figures 2 and 3) confirm the presence of the peptide fragment in the copolymer molecule and provide the determination of its content using the described technique.<sup>11</sup>

The NMR spectral bands characterize polymer overlap with many bands proper to peptides, but in the region of 4.2–4.5 ppm, wherein the polymer carrier has no signals, one can see a set of bands that might be attributed to proton signals of CH<sub>2</sub> in the pyrrolidone ring of the peptide (Figure 3). Besides, signals in the regions of 2.7–2.8 ppm and 2.97–2.99 ppm and in the region of 3.31 ppm were detected. These signals are absent in the spectra of the polymer and, thus, can be identified as signals of proton in the peptide.

The results of the SEC study (Table 1, Figure 4) demonstrate rather narrowed molecular weight distributions of the initial P4 and P4P copolymer. A light decrease in the block copolymer molecular weight might be explained by the fractioning of the polymer during purification via precipitation and dialysis.

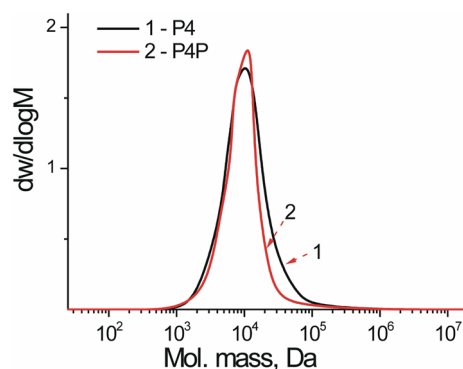


**Figure 4.** Molecular mass distributions for poly(PEGMA-co-DMM)-CGE (P4) and the SPS-peptide containing (P4P) copolymers.

Initial and resulting copolymers are polymeric surfactants soluble in water and forming in water solution micelle-like structures of Z-average hydrodynamic diameter in the range 180 ± 60 nm. It is evident (Table 1 and Figure 5) that the colloidal structures formed by pure peptide are characterized by a multimodal size distribution. The initial comb-like polymeric surfactant forms micelles of significantly less hydrodynamic diameter and of narrowed size distribution.

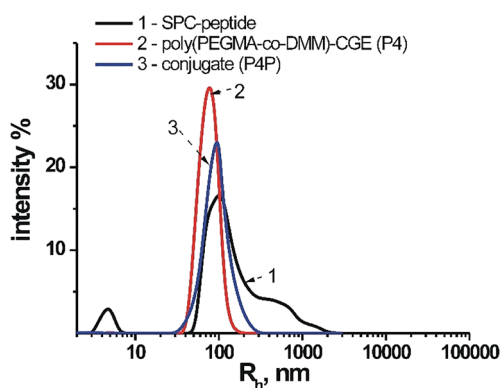


**Figure 5.** Hydrodynamic radii of the micelles formed in water by the SPC tripeptide (1), poly(PEGMA-*co*-DMM)-CGE (P4) (2), and conjugate poly(PEGMA-*co*-DMM)-CGE...SPC tripeptide (P4P) (3).

An increase in size and slight broadening of size distribution suggests the micelle-like structures formed by the SPC tripeptide containing copolymer. We consider that besides conjugated terminal fragment of the SPC tripeptide, the copolymer contains a certain amount of noncovalently bound peptide molecules.

**Effect of the SPC Tripeptide, P4 Polymer, and Their Conjugate (P4P) on Cell Viability *In Vitro*.** We applied MTT assay which allows quantitative measurement of the viability of treated cells as the level of activity of mitochondrial dehydrogenases in these cells. That was done in order to compare the cytotoxic action of three agents under study, namely, the SPC tripeptide (free form), the polymeric platform used for this peptide (free form), and the covalent conjugate of these substances. Two lines of tumor cells (human breast carcinoma cells of MCF-7 line and human colorectal carcinoma cells of HCT-116 line), pseudonormal cells of HEK-293 line from human embryo kidney, and normal CD3-positive lymphocytes (mononuclear cells of human peripheral blood) were treated with the aforementioned agents. Although

HEK-293 cells are widely used in biotechnology and toxicology research for comparison of the responses of the pathological (mostly tumor) and normal human cells to the action of stressing agents, and they are considered to be pseudonormal due to the ability of long-term growth and multiplication *in vitro*, their karyotype is abnormal and they are capable of forming tumors in the nude mice (atcc.org: 293[HEK-293]-CRL-1573/ATCC).

As one can see in Figure 6, all four types of human cells were found to be resistant to the action of free SPC tripeptide. The pseudonormal HEK-293 cells and normal CD3-positive lymphocytes were also resistant to the action of the free polymer, which, however, inhibited the viability of human tumor cells of the MCF-7 and HCT-116 lines. The viability of tumor cells (MCF-7 and HCT-116 lines) and pseudonormal cells (HEK-293) was significantly inhibited by the studied conjugate (P4P), while normal CD3-positive lymphocytes were totally resistant to such action.

Thus, for the investigation of the pro-apoptotic action of studied agents, the MCF-7 cells of human breast carcinoma were selected as tumor model cells that are the most sensitive to such action. These cells were used in the next experiments—fluorescent microscopy with FITC-Annexin V and propidium iodide, FACS analysis with FITC-Annexin V/propidium iodide, Western blot analysis of the apoptosis related proteins, fluorescent microscopy for study of the uptake of FITC-labeled P4P conjugate, and ROS measurement with fluorescent microscopy and FACS analysis using the DCFDA dye.

Cytotoxic effects of the SPC tripeptide, initial polymer and their conjugate toward human breast carcinoma cells of the MCF-7 line, human colon carcinoma cells of HCT116 line, and normal anti-CD3-activated lymphocytes of human peripheral blood were studied. The results of MTT assay of cell viability demonstrated that P4 polymer and P4P conjugate inhibited the viability of human tumor cells; however, there was no significant effect of the P4P toward viability of anti-

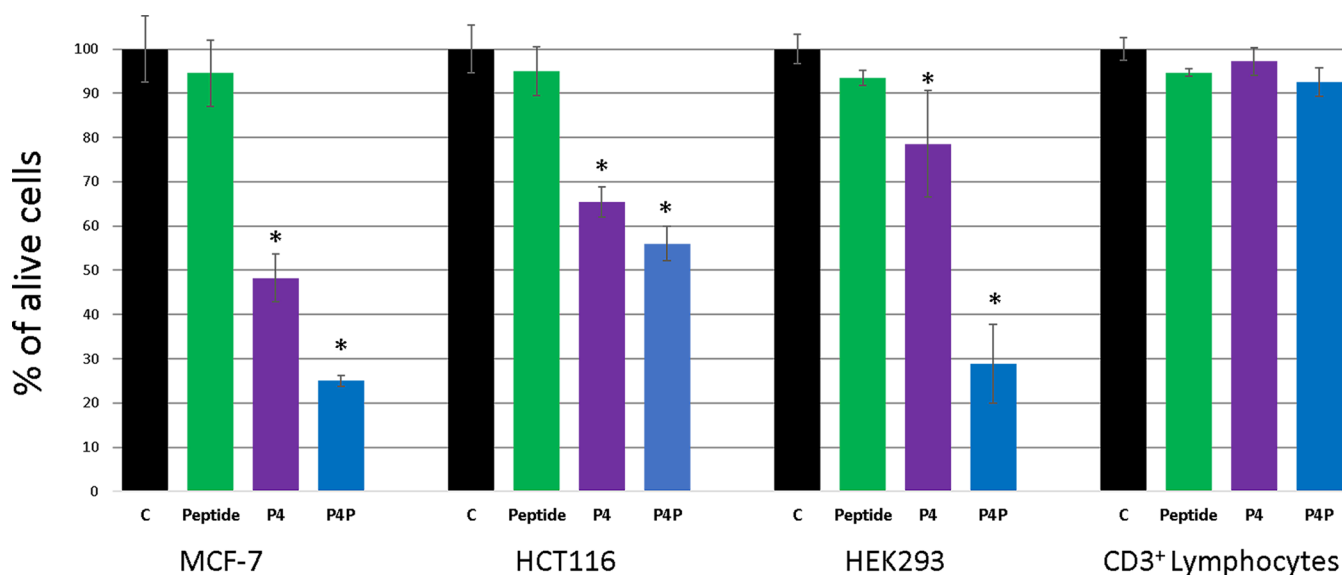


**Figure 6.** Effect of the P4P conjugate on the viability (MTT assay) of human breast carcinoma MCF-7 cells, human colon carcinoma HCT116 cells, and anti-CD3-activated normal lymphocytes of human peripheral blood. C – control (intact cells); Peptide – SPC tripeptide (0.13 mg/mL); P4 – P4 polymer (1.66 mg/mL); P4P – P4 polymer conjugated with SPC tripeptide (polymer – 1.66 mg/mL, SPC – 0.13 mg/mL). Treatment – 24 h.\* $P < 0.05$  compared to Control.

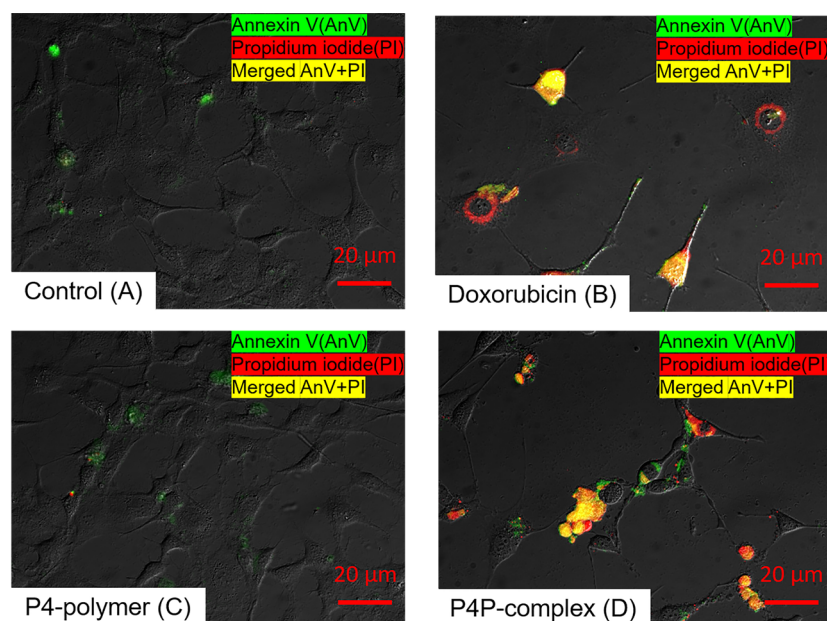


**Figure 7.** MCF-7 cells stained with FITC-Annexin V and propidium iodide: A – Control (untreated cells); B – Doxorubicin (1  $\mu\text{g}/\text{mL}$ ); C – P4 polymer (1.66 mg/mL), D – P4P (polymer – 1.66 mg/mL, SPC – 0.13 mg/mL). After 24 h treatment, the cells were stained with FITC-Annexin V and propidium iodide. FITC-Annexin V (phosphatidylserine marker in apoptotic cells) – green fluorescence, propidium iodide (marker of plasma membrane damage in dead cells) – red fluorescence, merging of FITC-Annexin V and propidium iodide signals – yellow-orange fluorescence.

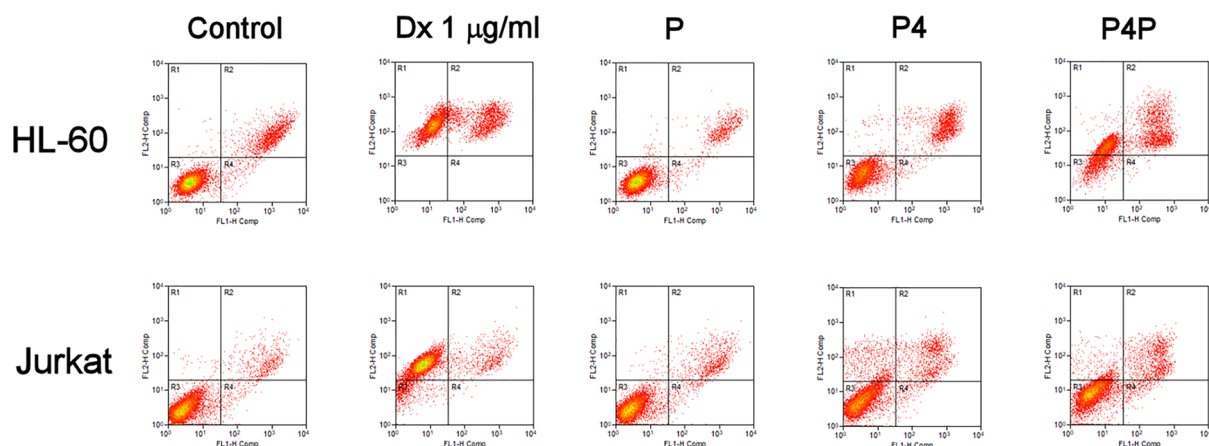


**Figure 8.** Results of flow cytometry analysis of cell death in human leukemia HL-60 cells and Jurkat cells treated for 24 h with Dx – Doxorubicin (1  $\mu\text{g}/\text{mL}$ ); P – SPC peptide (0.13 mg/mL); P4 – polymer without peptide (1.66 mg/mL); P4P – block/branched copolymer containing SPC tripeptide (polymer – 1.66 mg/mL, SPC – 0.13 mg/mL). Annexin V/PI double staining: R1-AnV(-)/PI(+), R2-AnV(+)/PI(+), R3-AnV(-)/PI(-), R4-AnV(+)/PI(-).

CD3-activated normal lymphocytes of human (Figure 6). Higher doses of tested compounds were not used in dose-dependence studies because that affected their stability and other physicochemical properties. In order to explain more pronounced cytotoxic effect of P4P toward human breast cancer cells of MCF-7 line and human colon carcinoma cells of HCT116 line, compared with the cytotoxic effect of P4P toward normal human lymphocytes, an additional investigation is necessary.

In future studies, we will use a wider panel of human tumor cells in order to approve if the anticancer action of the P4P conjugate is a universal characteristic of this novel killer of the tumor cells. We will also treat human CD3 lymphocytes for exploring whether cellular normality prevents the cytotoxic action of the P4P conjugate and studying which could be the

mechanisms of such prevention. The main goal of the present investigation was to demonstrate that chemical modification, like covalent conjugation of small molecules and SPC tripeptides with the high molecular weight polymer, both of which are tolerant to studied human cells, may lead to formation of their cytotoxic conjugate.

**Pro-Apoptotic Action of P4P Conjugate.** Three different approaches were applied in order to confirm the pro-apoptotic action of the P4P conjugate toward treated human cells: (1) fluorescence microscopy of cells with using FITC-Annexin V and propidium iodide staining; (2) flow cytometry with using the same fluorescent dyes; (3) Western-blot analysis of apoptosis-specific proteins in the treated cells.

**Fluorescence Microscopy.** Results demonstrated that P4P (polymer – 1.66 mg/mL, SPC – 0.13 mg/mL) induced the



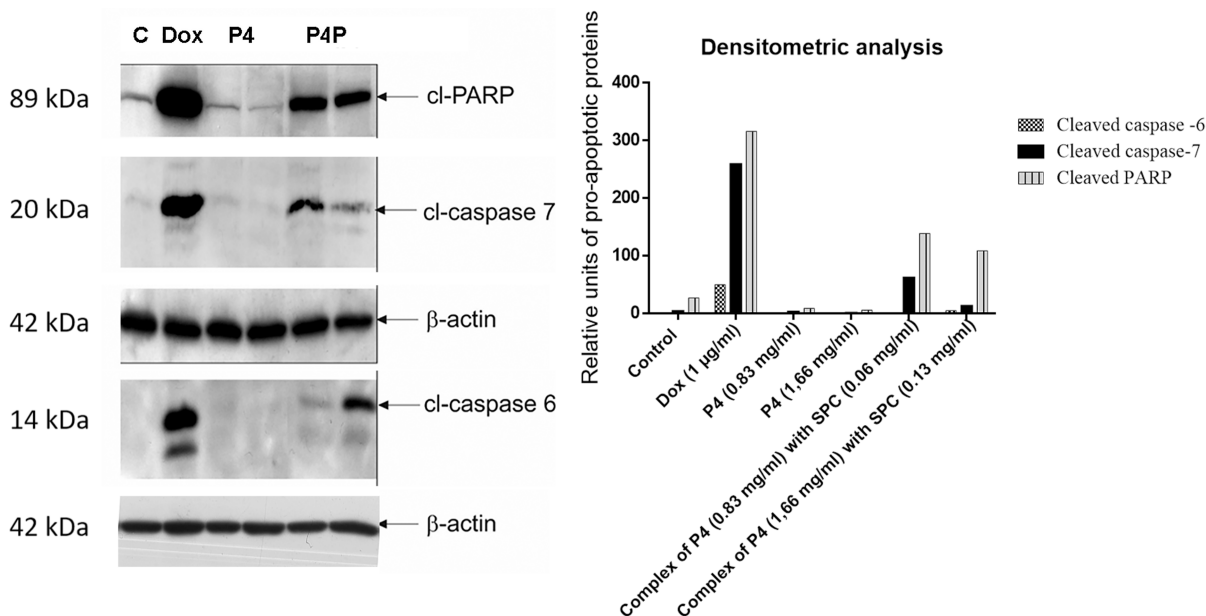


**Figure 9.** Results of Western blot analysis and blot densitometry for apoptosis-specific proteins in the MCF-7 cells. Lane 1 – intact cells (negative control); lane 2 – doxorubicin, 1  $\mu\text{g}/\text{mL}$  (positive control); lanes 3 and 4 – P4 polymer in concentration of 0.83  $\mu\text{g}/\text{mL}$  and 1.66  $\mu\text{g}/\text{mL}$ , respectively; lane 5 – P4P conjugate with concentration of polymer – 0.83  $\mu\text{g}/\text{mL}$  and SPC – 0.06  $\mu\text{g}/\text{mL}$ ; lane 6 – P4P conjugate with concentration of polymer – 1.66  $\mu\text{g}/\text{mL}$  and SPC – 0.13  $\mu\text{g}/\text{mL}$ .

pro-apoptotic effects in the treated human carcinoma cells of MCF-7 line (Figure 7A). The P4P increased the number of cells positive for FITC-Annexin V and propidium iodide staining (Figure 7D), compared to untreated cells (Figure 7A) and cells treated with free P4 polymer (Figure 7C). Similar pro-apoptotic effect was observed under the action of a known anticancer drug, doxorubicin (Figure 7B).

Fluorescence microscopy was applied with using Carl Zeiss AxioImager A1, 400 $\times$  magnification, Carl Zeiss Axio-CamMRm.

**Flow Cytometry.** In order to avoid potential false positive and false negative results which might be caused by a necessity of detaching the monolayer cells, like MCF7 or HCT116, in the conducted FACS analysis of the induced cell death, we purposely used a suspension of human cells of HL-60 and Jurkat T-leukemia lines that were treated with the tested compounds. HL-60 and Jurkat cells were stained with Annexin V and propidium iodide and then subjected to FACS analysis (Figure 8). We detected an elevated percentage of Annexin V-positive/propidium iodide negative (early apoptosis) and Annexin V-positive/propidium iodide positive (late apoptosis) HL-60 cells and Jurkat T-cells after their treatment with P4P conjugate, compared with the ratio of these cells treated with free peptide (P) or free polymer (P4). It should be stressed that at treatment of cells of both lines (HL60 and Jurkat) with a traditional anticancer medicine—doxorubicin—most of the treated cells were Annexin V-negative/propidium iodide-positive, which suggests necrosis (Figure. 8). These results suggest that the P4P conjugate possesses an apoptosis-inducing potential, while there was no pro-apoptotic effect of free peptide (P) and free polymer (P4), and results did not differ significantly from those in the control.

It is difficult to compare in a direct way the results of the MTT assay on measuring cell viability under P4 and P4P treatment (we cannot define the way of cell death taking into account the results of the MTT assay) with the results of

FACS analysis demonstrating the presence of some indicators of cell death. However, in both MTT assay and FACS analysis, the general tendencies revealed are the same, namely, free tripeptide is nontoxic, and P4P conjugate is definitely more toxic than free polymer (P4).

**Western Blot Analysis.** The involvement of apoptosis in the mechanisms of toxic action of the created P4P conjugate toward human tumor cells was confirmed by the results of Western blot analysis of apoptosis-specific proteins in the treated cells (Figure 9). Increased amounts of cleaved Poly(ADP-ribose) polymerase (PARP), as well as of Caspases 6 and 7, were detected in the MCF-7 cells under the action of both P4P conjugate (Figure 9, lanes 5, 6) and doxorubicin (positive control) (Figure 9, lane 2). At the same time, the level of these pro-apoptotic proteins in the MCF-7 cells treated with free polymer (Figure 9, lanes 3, 4) was close to the level found in the untreated cells (Figure 9, lane 1). Thus, the cytotoxic effect of P4P conjugate toward MCF-7 cells is realized via apoptosis mechanisms.

Apoptosis is characterized by numerous morphological changes in the cell, as well as changes in biochemical processes which depend on the activity of several specific enzymes.<sup>14</sup> The Western blot analysis of proteins involved in the initiation and execution of apoptosis and in regulation of cell cycling is a common approach used in studies of the molecular mechanisms of the effects of various anticancer drugs. At the action of these drugs toward tumor cells, the cleavage of the DNA reparation enzyme—Poly(ADP-ribose) polymerase (PARP)—takes place. That leads to inactivation of PARP and cell death through apoptosis, because the DNA reparation is blocked.<sup>15</sup> Caspases are the hydrolytic enzymes which participate in fragmentation of PARP, as well as in cleavage of other regulatory proteins in cells induced to apoptosis. Opposite to PARP, partial cleavage of caspases leads to their activation.<sup>16</sup>

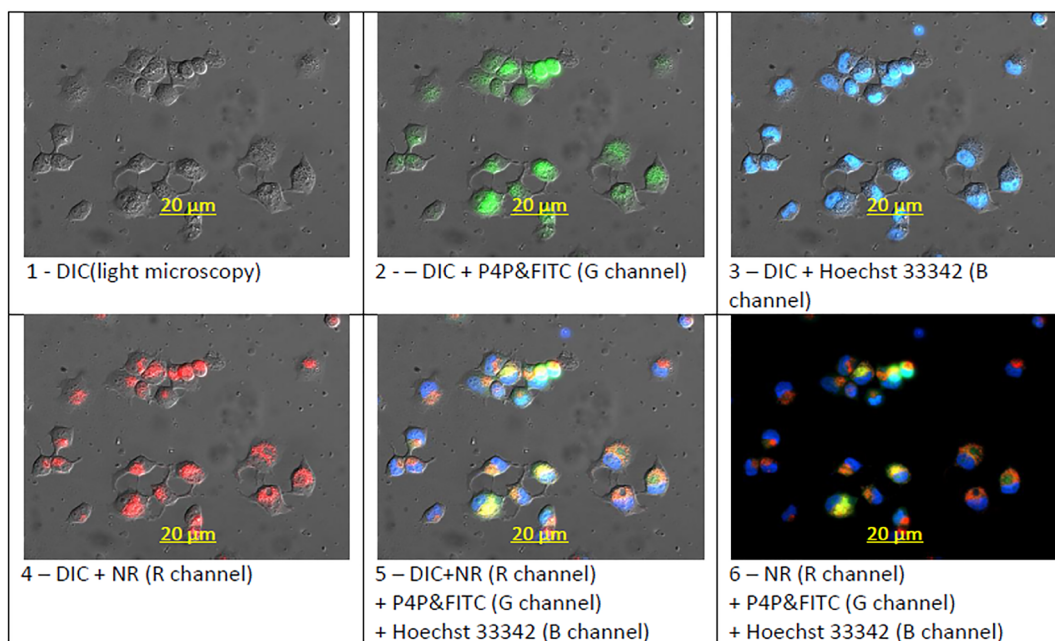


**Figure 10.** Localization of P4P-FITC conjugate which penetrated into MCF-7 cells. 1 – DIC image (light microscopy); 2 – green fluorescence of engulfed FITC-labeled P4P conjugate; 3 – blue fluorescence due to binding of Hoechst-33342 with the DNA; 4 – red fluorescence due to neutral red engulfment by the lysosomes of the alive (not dead) cells; 5 – merged cell staining with FITC-P4P, Hoechst-33342, and neutral red on DIC image; 6 – merged cell staining with FITC-P4P, Hoechst-33342, and neutral red without DIC image; P4P – FITC labeled polymer was conjugated with the SPC tripeptide (polymer – 1.66 mg/mL, SPC – 0.13 mg/mL), 400 $\times$  magnification.

It is known that Caspase-3, -6, and -7 belong to the executioner caspases which destroy several important intracellular proteins, such as fodrin, gelsolin, U1 small nuclear ribonucleoprotein, DNA fragmentation factor 45 (DFF45), receptor-interacting protein (RIP), X-linked inhibitor of apoptosis protein (X-IAP), signal transducer and activator of transcription-1 (STAT1), topoisomerase I, vimentin, Rb, and lamin B.<sup>17</sup> While the caspase-9 acts as an initiator caspase in the intrinsic apoptosis pathway, in the caspase cascade, caspase-9 cleaves and activates caspase-7.

As one can see on Figure 9, a similar tendency is observed in dose dependence changes in the amount of the Caspase-7 (a decrease from 62 to 13 relative units) and in the amount of the PARP (a decrease from 139 to 109 relative units) which is a substrate of the Caspase-7 in the apoptosis pathway.<sup>17</sup> At the same time, a dose dependent dynamics of change in the amount of the Caspase-6 is opposite (an increase from 1 to 50 relative units) to such dynamics in the Caspase-7 (see above). The regulation of the activity of the caspase-6 differs significantly from that of the caspase-7, since Caspase-6 is first split and activated by the executioner caspase-3 and then starts its destructive action in the cell.<sup>17</sup>

**P4P Conjugate Penetrates into Human Tumor Cells *in Vitro*.** We investigated whether P4P conjugate is capable of penetrating into the mammalian cells. To do that, P4P was covalently labeled with the fluorescent dye, FITC, and the interaction of P4P-FITC with MCF-7 cells was studied by means of the fluorescent microscopy (Figure 10).

After treatment of the MCF-7 cells for 2 h with FITC-labeled P4P conjugate, this material was detected in the targeted cells (Figure 10, image 2). Blue fluorescence of nuclear chromatin stained with Hoechst-33342 was localized in treated cells separately from red fluorescence of lysosomes and green fluorescence of FITC-P4P, both observed in cellular cytosol (Figure 10, image 5). The only overlapping of

fluorescence colors was detected when cells were stained simultaneously with FITC, Hoechst-33342, and neutral red (Figure 10, image 6). In this case, the green fluorescence of FITC interfered with the red fluorescence of the neutral red to give a yellow-orange color, since lysosomes are located in cellular cytosol. Thus, the cytotoxic location of P4P conjugate in the MCF-7 cells suggests the penetration of this conjugate into the treated cells. Additional experiments are needed to answer the question of whether P4P conjugate is transported to lysosomes and if the bioactive products of its degradation appear or it fulfills its biological role as an apoptosis inducer when it stays in the cytosol. The localization of the P4P conjugate in the lysosomes might lead to its degradation or might render the conjugate inactive since the lysosomal pH is highly acidic. At present, we do not have a distinct answer regarding how the conjugate enables a pro-apoptotic effect in the tumor cells after it gets inside the lysosomes.

An enhanced permeability and retention (EPR) effect is an important mechanism which should be taken into consideration at the design of novel medicines. It is dependent upon several endogenous and exogenous factors appearing in tumors.<sup>18</sup> Due to this effect, molecules of free form of the drug are rapidly released from tumor tissue, while its form immobilized on the particles is retained in tumor for a longer time.

Besides, the EPR effect can improve a therapeutic action of anticancer drugs, as well as decrease their general toxicity in the organism. While passive targeting of free drug shows only few minutes of the retention time, due to the EPR effect, the medicines encapsulated into nanoparticles demonstrate a retention time with days to weeks duration.<sup>19</sup>

Thus, it might be suggested that the P4P conjugate which exists as a nanoparticle (see Table 1) will be more effective in treatment of tumor bearing animals, compared with low-

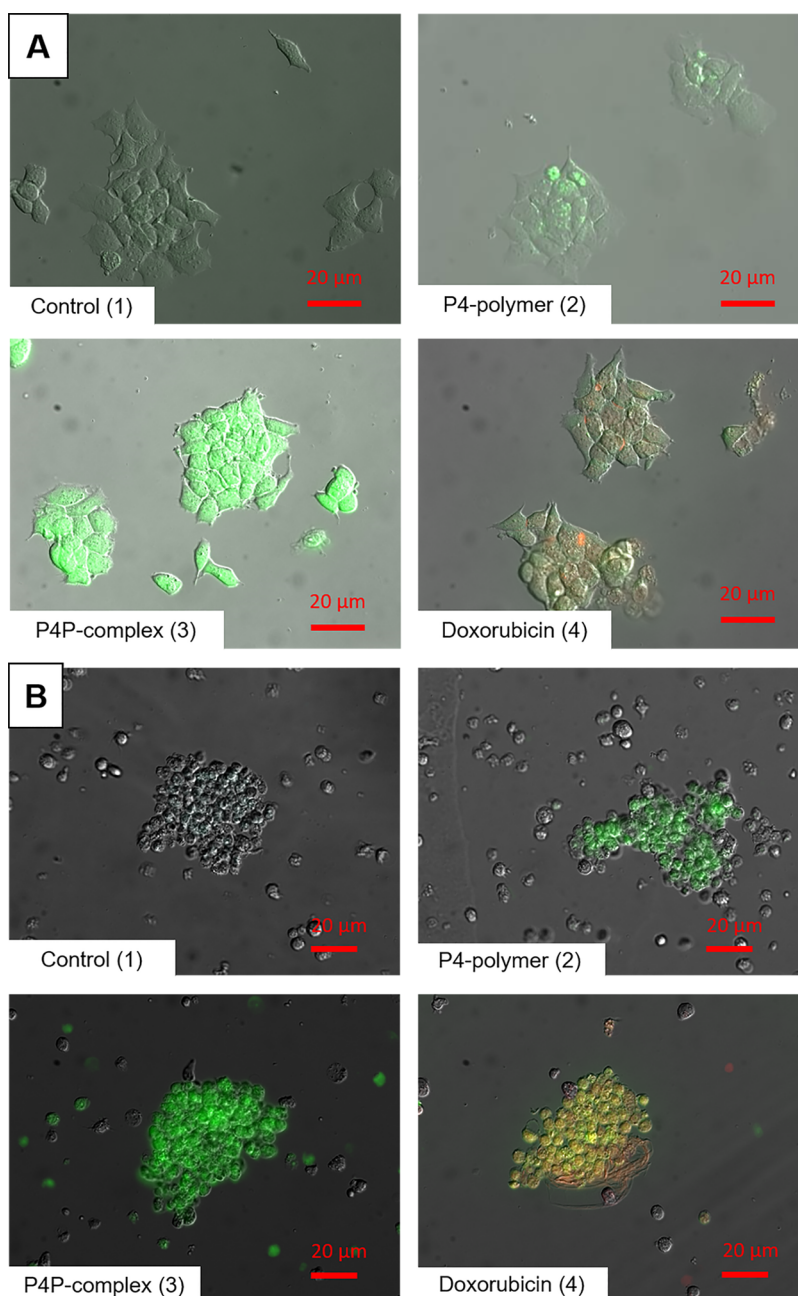


**Figure 11.** Results of ROS measurement with 2,7-dichlorofluorescein diacetate (DCFDA) in the MCF-7 cells (A) and Jurkat cells (B) treated for 30 min with free P4 polymer or P4P conjugate: 1 – Control (untreated cells); 2 – P4 treatment (free polymer, 130  $\mu\text{g}/\text{mL}$ ); 3 – P4P treatment (polymer conjugated with the SPC tripeptide, 130  $\mu\text{g}/\text{mL}$ ); 4 – Doxorubicin treatment (Dox, 1  $\mu\text{g}/\text{mL}$ ). 400 $\times$  magnification.

molecular-weight free SPC tripeptide which did not show any activity in all assays used in our study.

**Induction of ROS Generation by the P4P Conjugate in the MCF-7 Cells.** An excessive production of the reactive oxygen species (ROS) is known to cause cell damage and apoptosis.<sup>20</sup> We applied ROS-sensitive DCFDA fluorescent dye which detects mainly  $\text{H}_2\text{O}_2$  in order to monitor the oxidative stress in the treated cells.

The results of fluorescent microscopy demonstrated an increased ROS content in P4P-treated cells (Figure 11, image 3 in sections A and B), compared with P4-treated MCF-7 cells (Figure 11, image 2 in sections A and B). Thus, the cytotoxic (pro-apoptotic) effect of the P4P conjugate toward human breast carcinoma cells of the MCF-7 line might be linked to

the elevated production of ROS in these cells. Some level of ROS production was also found at treatment of both tumor cell lines (MCF-7 and Jurkat) with free polymer P4 (Figure 11, image 2 in sections A and B). In the image 4 (Figure 11, in sections A and B) of doxorubicin action, there was nice merging of green fluorescence of the DCFDA with red fluorescence of the doxorubicin. These data correspond to the results of cell viability study (MTT assay) presented in Figure 5. Those results did not reveal the cytotoxicity of free form of the SPC tripeptide, while there was some cytotoxicity of free form of the polymer P4, of course, much lower than the cytotoxicity of the conjugate P4P.

On Figure 12, ROS production in the treated MCF-7 cells was also measured using FACS analysis. As one can see, ROS



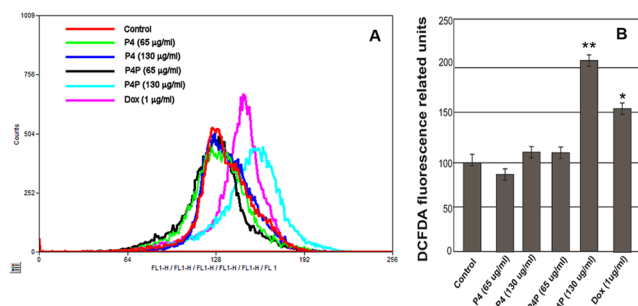


**Figure 12.** Results of ROS measurement with 2,7-dichlorofluorescein diacetate (DCFDA) by FACS analysis using flow cytometry (BD Biosciences, Mountain View, CA) in the MCF-7 cells treated for 30 min with free P4 polymer or P4P conjugate: Control (untreated cells); P4 treatment (free polymer, 65 and 130  $\mu\text{g/mL}$ ); P4P treatment (polymer conjugated with the SPC tripeptide, 65 and 130  $\mu\text{g/mL}$ ); Doxorubicin (Dox, 1  $\mu\text{g/mL}$ ) treatment. A – original patterns of FACS analysis, B – quantitative presentation of the results of FACS analysis.

level was increased at 130  $\mu\text{g/mL}$  dose of the P4P conjugate, similar to what was found in the evaluation of ROS level by means of the fluorescent microscopy (Figure 11). However, there was no significant increase of ROS level under the action of higher doses of P4 polymer.

Ser-Pro-Cys (SPC) tripeptide was first detected by us in the blood serum of multiple sclerosis patients.<sup>1</sup> However, up to now its biological role remained unknown. In this study, we addressed this issue in more detail. To reach this goal, a synthetic analogue of the SPC tripeptide was obtained in order to have the possibility to work with a sufficient amount of peptide material. Its effect *in vitro* on the viability of tumor and normal human cells was investigated. The SPC-tripeptide was covalently conjugated to the PEGylated comb-like polymer, and the created conjugate demonstrated a significant cytotoxic action (MTT assay) toward human tumor cells. However, it did not affect the viability of normal cells, namely, activated lymphocytes of the peripheral blood of healthy human donors.

Summarizing, we consider that the created P4P conjugate might be a platform for novel antitumor medicine that consists of two biocompatible nontoxic components—SPC tripeptide and PEGylated comb-like polymer. This hybrid conjugate penetrates into tumor cells, localizes in their cytosol, triggers elevation of ROS content in treated cells, and induces their apoptosis. A search for potential intracellular protein targets of the SPC tripeptide conjugated with the polymer (P4P) is in progress. The resistance of normal lymphocytes of the peripheral human blood to the action of the created conjugate, compared with its cytotoxic action toward human tumor cells, is of great interest. The action of the P4P conjugate in the laboratory tumor-bearing mice will be also studied.

## CONCLUSIONS

Physico-chemical characteristics (hydrodynamic diameter of the obtained polymeric micelles, <sup>1</sup>H-NMR spectra of their complexes with SPC tripeptide, elemental composition, and zeta potential) of the synthesized polymeric complexes were defined. FITC-labeled conjugate of these polymeric structures was prepared and used for targeting tumor cells. The penetration of this conjugate functionalized with covalently immobilized SPC tripeptide into the targeted cells and its ability to induce intracellular generation of ROS and cause cell

death (apoptosis) were monitored. It should be noted that covalent conjugate of the SPC-peptide with PEGylated polymer possessed cytotoxic activity toward human tumor cells *in vitro*, while the activated normal lymphocytes of the peripheral blood of human donors were resistant to such action. The created conjugate penetrated into target tumor cells, accumulated in their cytoplasm, and triggered ROS production that was accompanied by the induction of apoptosis. The presented data provide a new insight on the potential biological role of the Ser-Pro-Cys tripeptide. The created conjugate may serve as a platform for development of new type of the biocompatible, antitumor medicine.

## AUTHOR INFORMATION

### Corresponding Author

Rostyslav Stoika – Institute of Cell Biology, NAS of Ukraine, Lviv 79005, Ukraine; Email: [stoika.rostyslav@gmail.com](mailto:stoika.rostyslav@gmail.com)

### Authors

Nazar Manko – Institute of Cell Biology, NAS of Ukraine, Lviv 79005, Ukraine; [orcid.org/0000-0003-1203-7479](https://orcid.org/0000-0003-1203-7479)

Marina Starykovich – Institute of Cell Biology, NAS of Ukraine, Lviv 79005, Ukraine

Nataliya Mitina – Lviv National Polytechnic University, Lviv 79000, Ukraine

Kateryna Volianiuk – Lviv National Polytechnic University, Lviv 79000, Ukraine

Lizhen Wang – Biology Institute of Shandong Academy of Sciences, Jinan 250014, People's Republic of China

Meng Jin – Biology Institute of Shandong Academy of Sciences, Jinan 250014, People's Republic of China; [orcid.org/0000-0002-1525-0876](https://orcid.org/0000-0002-1525-0876)

Kechun Liu – Biology Institute of Shandong Academy of Sciences, Jinan 250014, People's Republic of China; [orcid.org/0000-0001-5461-5818](https://orcid.org/0000-0001-5461-5818)

Rostyslav Panchuk – Institute of Cell Biology, NAS of Ukraine, Lviv 79005, Ukraine

Olga Klyuchivska – Institute of Cell Biology, NAS of Ukraine, Lviv 79005, Ukraine

Alexander Zaichenko – Lviv National Polytechnic University, Lviv 79000, Ukraine; [orcid.org/0000-0002-7742-1984](https://orcid.org/0000-0002-7742-1984)

Yuriy Kit – Institute of Cell Biology, NAS of Ukraine, Lviv 79005, Ukraine

Complete contact information is available at:

<https://pubs.acs.org/10.1021/acsomega.2c03611>

### Notes

The authors declare no competing financial interest.

## ACKNOWLEDGMENTS

The authors thank prof. Maxim Lootsik and Dr. Nataliya Finiuk for their technical assistance during conducting experiments on cell treatments. Prof. Kechun Liu helped in purchasing the SPC tripeptide used in this study. There was no special financial support at performing this work.

## DEDICATION

In Memoriam: This manuscript was prepared in memory of prof. Yuriy Kit who was its first corresponding author. However, final editorial changes and paper submission were not possible because of sudden death of Yuriy Kit in the age of 62 caused by an acute heart attack. The coauthors of this

manuscript express their sincere pity of this loss and great respect to Yury Kit as a creative scientist and great colleague and friend.

## REFERENCES

- (1) Myronovkij, S.; Negrych, N.; Nehrych, T.; Tkachenko, V.; Souchelnyskyi, S.; Stoika, R.; Kit, Y. Identification of SER-PRO-CYS Peptide in Blood Serum of Multiple Sclerosis Patients. *Prot. Pept Lett.* **2016**, *23* (9), 808–811.
- (2) Ashford, M. B.; England, R. M.; Akhtar, N. Highway to Success - Developing Advanced Polymer Therapeutics. *Advanced Therapeutics* **2021**, *4* (5), 2000285.
- (3) Karabasz, A.; Bzowska, M.; Szczepanowicz, K. Biomedical Applications of Multifunctional Polymeric Nanocarriers: A Review of Current Literature. *Int. J. Nanomedicine.* **2020**, *15*, 8673–8696.
- (4) Ferreira Soares, D. C.; Domingues, S. C.; Viana, D. B.; Tebaldi, M. L. Polymer-hybrid nanoparticles: Current advances in biomedical applications. *Biomedicine & Pharmacotherapy* **2020**, *131*, No. 110695.
- (5) Appiah, E.; Nakamura, H.; Pola, R.; Grossmanová, E.; Lidický, O.; Kuniyasu, A.; Etrych, T.; Haratake, M. Acid-responsive HPMA copolymer-bradykinin conjugate enhances tumor-targeted delivery of nanomedicine. *J. Controlled Release* **2021**, *337* (10), 546–555.
- (6) Tang, H.; Tang, J.; Shen, Y.; Guo, W.-X.; Zhou, M.; Wang, R.-H.; Jiang, N.; Gan, Z.-H.; Yu, Q.-S. Comb-like Poly(N-(2-hydroxypropyl) methacrylamide) Doxorubicin Conjugates: The Influence of Polymer Architecture and Composition on the Biological Properties. *Chinese Journal of Polymer Science* **2018**, *36*, 1225–1238.
- (7) Kobylinska, L.; Patereha, I.; Finiuk, N.; Mitina, N.; Riabtseva, A.; Kotsyumbas, I.; Stoika, R.; Zaichenko, A.; Vari, S. Comb-like PEG-containing polymeric composition as low toxic drug nanocarrier. *Cancer Nanotechnology.* **2018**, *9* (1), 1 DOI: 10.1186/s12645-018-0045-5.
- (8) Paiuk, O. L.; Mitina, N. Y.; Kinash, N. I.; Yakymovych, A. B.; Hevus, O. I.; Zaichenko, A. S. Comb-like polyethylene glycol containing oligomeric surfactants with reactive terminal groups. *Ukr. Chem. J.* **2018**, *84* (10), 98–106.
- (9) Mitina, N.; Riabtseva, A.; Paiuk, O.; Finiuk, N.; Slouf, M.; Pavlova, E.; Zaichenko, A. Molecular Design, Synthesis, and Properties of Surface-Active Comb-Like PEG-Containing Polymers and Derived Supramolecular Structures for Drug Delivery. In *Biomedical Nanomaterials*, Stoika, R. S., Ed.; Springer: Cham, 2022. DOI: 10.1007/978-3-030-76235-3\_2.
- (10) Mitina, N. Y.; Riabtseva, A. O.; Garamus, V. M.; Lesyk, R. B.; Volyanyuk, K. A.; Izhyk, O. M.; Zaichenko, O. S. Morphology of the micelles formed by a comb-like PEG-containing copolymer loaded with antitumor substances with different water solubilities. *Ukrainian Journal of Physics* **2020**, *65* (8), 670.
- (11) Chen, C.; Ng, D. Y. W.; Weil, T. Polymer Bioconjugates: Modern Design Concepts Toward Precision Hybrid Materials. *Prog. Polym. Sci.* **2020**, *105*, 101241.
- (12) Volianiuk, K.; Mitina, N.; Kinash, N.; Harhay, K.; Dolynska, L.; Nadashkevich, Z.; Hevus, O.; Zaichenko, A. Telechelic Oligo(N-Vinylpyrrolidone)s with Cumene Based Terminal Groups for Block-Copolymer and Nanoparticle Obtaining. *Chemistry & Chemical Technology* **2022**, *16* (1), 34–41.
- (13) Mahmood, T.; Yang, P. C. Western blot: technique, theory, and trouble shooting. *N. Am. J. Med. Sci.* **2012**, *4* (9), 429–434.
- (14) D'Arcy, M. S Cell death: a review of the major forms of apoptosis, necrosis and autophagy. *Cell Biol. Int.* **2019**, *43* (6), 582–592.
- (15) Morales, J.; Li, L.; Fattah, F. J.; Dong, Y.; Bey, E. A.; Patel, M.; Gao, J.; Boothman, D. A. Review of poly (ADP-ribose) polymerase (PARP) mechanisms of action and rationale for targeting in cancer and other diseases. *Crit Rev. Eukaryot Gene Expr.* **2014**, *24* (1), 15–28.
- (16) Kesavardhana, S.; Malireddi, R.K. S.; Kanneganti, T.-D. Caspases in Cell Death, Inflammation, and Pyroptosis. *Annu. Rev. Immunol.* **2020**, *38*, 567–595.
- (17) Slee, E. A.; Adrain, C.; Martin, S. J. Executioner Caspase-3, -6, and -7 Perform Distinct, Non-redundant Roles during the Demolition Phase of Apoptosis. *J. Biol. Chem.* **2001**, *276* (10), 7320–7326.
- (18) Iyer, A. K.; Khaled, G.; Fang, J.; Maeda, H. Exploiting the enhanced permeability and retention effect for tumor targeting. *Drug Discovery Today.* **2006**, *11* (17–18), 812–818.
- (19) Maeda, H.; Nakamura, H.; Fang, J. The EPR effect for macromolecular drug delivery to solid tumors: Improvement of tumor uptake, lowering of systemic toxicity, and distinct tumor imaging in vivo. *Adv. Drug Delivery Rev.* **2013**, *65* (1), 71–79.
- (20) Redza-Dutordoir, M.; Averill-Bates, D. A. Activation of apoptosis signalling pathways by reactive oxygen species. *Biochimica et Biophysica Acta (BBA) -Molecular Cell Research.* **2016**, *1863* (12), 2977–2992.